A Laboratory Study of the Wakes of Ionospheric Satellites

S. D. Hester* and Ain A. Sonin†
Massachusetts Institute of Technology, Cambridge, Mass.

A steady-state plasma wind tunnel is described in which most of the similarity parameters governing the flow around ionospheric satellites can be reproduced. A study is presented of the wakes of bodies (mostly spheres) with dimensions ranging from comparable with the Debye length to large compared with the Debye length. No magnetic field was applied in these experiments. The measurements of near wakes agree in essence with available theory and/or previous experiment. The far wakes of spheres were found to have a wavelike character which was largely independent of body potential.

I. Introduction

In its passage through the earth's ionosphere, a satellite causes a disturbance in the local ionospheric electron and ion densities. The main part of this disturbance extends downstream of the satellite in the form of a diverging wake, in the interior of which the electron and ion densities differ from their undisturbed values.[1]

The structure of this disturbance is of interest for several reasons. Measurements of geophysical properties with satellite-borne instrumentation must be interpreted with due regard to the perturbation caused by the satellite itself.[2] Indeed, since the disturbance is sensitive to the local ionospheric properties, it is possible that some of those properties may be inferred from measurements of the disturbance structure, as for example in the experiments of Samir and Wrenn.[3] A knowledge of the wake structure is also necessary for the understanding of radiowave scattering measurements.[1,4] Finally, the problem is of fundamental interest since it involves many of the basic processes that occur in rarefied plasmas.

The properties of the ionospheric plasma through which a satellite travels have been discussed elsewhere.[1] At altitudes above about 200 km, the flow over a satellite is collision-free. Only at very large distances downstream can collisions influence the wake structure. At altitudes between about 200 and 1000 km, the satellite speed U is large compared with the ion thermal speed $\bar{c}_i$, but small compared with the electron thermal speed $\bar{c}_e$. At higher altitudes the ion thermal speed becomes comparable to the satellite speed. The Debye length is of the order of a few centimeters, which is small compared with the dimensions of a typical satellite but comparable, for example, to the radius of an antenna or instrument boom.

The similarity parameters which govern this problem are well established.[1] These are 1) the speed ratio based on the ion wave speed $U(kT_e/m_i)^{-1/2}$, 2) the ratio of the body radius to the Debye length a/λ_D, 3) the dimensionless body potential $e\phi_\sigma/kT_e$ (where ϕ_σ is the potential of the body with respect to the plasma), and 4) the ratio of ion to electron temperature T_i/T_e. Typical ionospheric values of these parameters are given in Table 1. The geomagnetic field introduces two more parameters: 5) the ratio of the body size to the electron gyro radius, and 6) the ratio of the body size to the ion gyro radius.

Previous work in this area has been discussed in the monograph by Al'pert, Gurevich, and Pitaevskii[1] and later by de-Leeuw.[5] The complexity of the governing equations (Vlasov's equation applied to the electrons and ions, coupled by Poisson's equation, with appropriate boundary conditions specified at the satellite surface) is such that a unified analysis has so far not been attempted. A large fraction of the available theoretical work applies to the case of no magnetic field,[1,6–16] and much of it incorporates various further simplifications. Some approximate analyses have, however, been presented which take into account the influence of the geomagnetic field on the wake structure.[1,17–19]

All the laboratory simulation experiments published to date have been performed in the absence of an applied magnetic field.[20–25] The experiments have confirmed qualitatively the features of the wake structure predicted by available theory. Perhaps the most detailed comparison has been carried out by Maslennikov and Sigov,[12] who performed numerical computations of wake structure for the conditions of Skvortsov and Nosachev's[23] laboratory experiments. The agreement was found to be reasonably good, but the comparison was somewhat clouded by the suspected presence of slow secondary ions in the test facility. The same experimental difficulty has hampered other attempts at laboratory simulation. Some field measurements from satellites and spacecraft are also available,[26–28] and show qualitative agreement with theory where a comparison can be made. However, the relative inflexibility and cost of such experiments do not make them a substitute for a successful laboratory simulation.

In this paper, we report a series of wake measurements which were carried out in a steady-state plasma wind tunnel with no applied magnetic field. Special care was taken to minimize the background density of slow secondary ions. As indicated in Table 1, the conditions available in the wind tunnel are such that most (but not all) of the similarity parameters for typical satellite-ionosphere interactions are reproduced, for large bodies as well as small bodies like antennas or Langmuir probes.

The wind tunnel and instrumentation are described in Sec. 2, and the data on the wakes of bodies of strip, cylindrical, and spherical shapes (mostly the latter) are discussed in Sec. 3. A study of the wakes of small wires is reported in a separate paper,[29] as is a study of Langmuir probe response under ionospheric flow conditions.[30]

Some points are to be noted in relating the present data to actual ionospheric flow conditions. First, all the results are for the case of no applied magnetic field. Secondly, most (but not all) experiments were done with a "cold ion" plasma in which $T_i/T_e \ll 1$. These conditions are strictly speaking inappropriate for modelling a real satellite wake. A magnetic field would lead to fundamental differences in the sufficiently far wake, and hotter ions would result in stronger damping of the wake features than is observed in most of the present mea-

Received June 1969; revision received December 24, 1969. This material was presented in Paper 69-673 at the AIAA Fluid and Plasma Dynamics Conference, San Francisco, June 16–18, 1969. The research was supported by the Advanced Research Projects Agency (Ballistic Missile Defense Office) and technically administered by the Fluid Dynamics Branch of the U. S. Office of Naval Research under Contract NONR-1841 (93).

* Research Assistant, Department of Mechanical Engineering; now at Avco Everett Research Laboratory, Everett, Mass.

† Associate Professor, Department of Mechanical Engineering.

surements. Finally, we note that the experiments were performed in a somewhat source-like flow, as discussed below, rather than in a uniform freestream. The results are, however, felt to be of fundamental interest and should be useful for comparison with theoretical models.

2. Plasma Wind Tunnel, Flow Conditions, and Instrumentation

The plasma wind tunnel is a steady-state flow facility in which a collision free plasma beam is produced by extraction and electrostatic acceleration of argon ions from a plasma source. The system (Fig. 1) consists of a 20-in.-diam cylindrical vacuum chamber which houses the plasma source and an instrument carriage for probing the flowfield around models in the stream. A 20-in. diffusion pump with 18000 liter/sec capacity maintains the chamber pressure at about 10^{-5} torr under operating conditions. The facility can produce a broad range of plasma flow conditions (ion number density from 10^6 – 10^8 cm^{-3}, electron temperature from 4000–60,000°K, flow speed from 1.5 to 15 cm/μsec) covering ionospheric flow conditions in terms of the relevant similarity parameters (Table 1).

The plasma source (Fig. 2) is based on the design of an electron bombardment ion rocket,[31] as in the facility used by Clayden and Hurdle.[22] Argon was used as the working gas. The gas is admitted to a cylindrical ionization chamber where a plasma is produced by means of a discharge between the hot cathode on the chamber axis and an anode which forms the circumference of the chamber. An axial magnetic field of the order of ten gauss is applied to allow the discharge to operate at as low a pressure as possible. A negatively biased grid (2.5- to 20-cm diam grids were employed) at one end of the ionization chamber extracts ions from the plasma and accelerates them to a high velocity as the ions drop through the potential difference between the plasma in the ionization chamber and the plasma stream.

The ion stream emerging from the source is neutralized by a background of electrons supplied either from hot filaments in the stream or from the source itself. The hot filaments, biased several volts positively relative to all surfaces in contact with the plasma in order to retain the emitted electrons in the stream, were used when low electron temperatures (of the order of the filament temperature) were desired. A hotter electron background ($kT_e/e > 1$ ev) was obtained when the background electrons were drawn from the source itself. In this mode, the source cathode potential was made slightly negative with respect to the accelerator grid (Fig. 2) so that electrons could escape, and an equilibrium was established with the stream plasma potential somewhat positive with respect to the source cathode. The higher electron temperature mode was used in order to achieve the lower values of the speed ratio $U(kT_e/m_i)^{-1/2}$. Very nearly Maxwellian electrons were obtained with both neutralizing modes.

Point measurements of ion density, electron temperature, and plasma potential were made with Langmuir probes. Surveys of ion density were obtained with probes biased at a fixed negative potential, and continuous surveys of plasma potential were obtained with emissive probes.

Table 1 Values of similarity parameters

Parameter	Ionosphere	Plasma wind tunnel
$U(kT_e/m_i)^{-1/2}$	30 at 100 km altitude, decreasing to 2 at 3000 km altitude	5-100
a/λ_D	<1 for antenna or probe $>10^2$ for satellite body	10^{-2}–10^2
$e\phi_\sigma/kT_e$	-7 to ~ 0	externally controlled
T_i/T_e	$\frac{1}{2}$ – 1	10^{-3} – 1

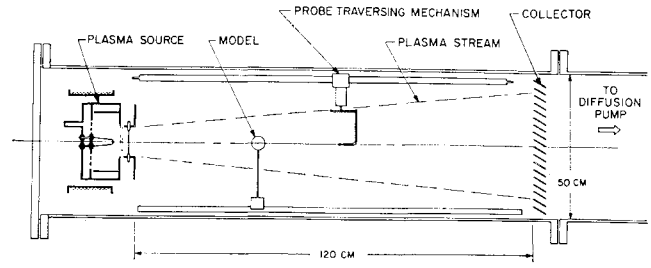

Fig. 1 Plasma wind tunnel.

For ion density measurement, cylindrical probes with their axes transverse to the flow were used in the wakes of two-dimensional bodies such as cylinders and strips, and spherical probes were used in the wakes of spheres. The probe size was small compared with the body size in all cases. The response of collision-free Langmuir probes has been discussed elsewhere.[32,33] For a negatively biased probe small compared with the Debye length in a high-speed flow [$U(kT_e/m_i)^{-1/2} \gg 1$], the relationship between the total ion current I and the local ion density n is particularly simple.[32] For a cylindrical probe transverse to the flow,

$$I = enU2r_pL(1 + e|\phi_p|/\tfrac{1}{2}m_iU^2)^{1/2} \qquad (1)$$

and for a spherical probe

$$I = enU\pi r_p^2(1 + e|\phi_p|/\tfrac{1}{2}m_iU^2) \qquad (2)$$

Here, e is the electronic charge, U is the flow speed, r_p is the probe radius, L is the probe length in the case of a cylindrical probe, ϕ_p is the (negative) probe potential relative to the plasma, and m_i is the ion mass. Equations (1) and (2) were used to determine the ion density from the probe current once the plasma potential and the flow speed had been established (see below). The ion density distributions in the wakes were obtained by making surveys of ion current with probes at fixed negative potential. Since U was virtually constant in each wake, the ion current at fixed probe potential was simply proportional to ion number density.

The electron temperature was obtained from the probe characteristics by the conventional method[32,33] of plotting the logarithm of the electron current vs the probe potential. The electron energy distribution was to a good approximation Maxwellian, and the electron temperature was essentially uniform in the test section.

The plasma potential was determined from the characteristics of conventional probes[33] and also with an emissive probe.[32] (The emissive probe proved convenient for making continuous mappings in model wakes.)

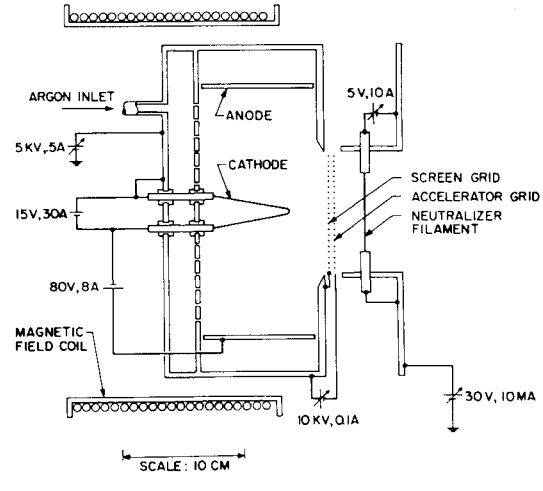

Fig. 2 Plasma source.

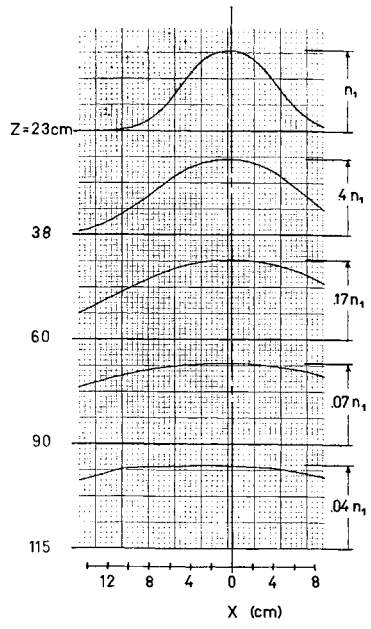

Fig. 3 Profiles of ion density in plasma stream from an accelerator grid of 1.27 cm radius; $n_1 = 1.4 \times 10^8$ cm^{-3}.

The flow speed U of the stream ions was calculated on the assumption that the accelerating potential was the difference between the source anode potential and the local plasma potential measured in the stream (measurements showed the plasma within the source to follow the anode potential). A time-of-flight measurement provided a direct verification of this velocity (to an accuracy better than 10%) and a repelling potential energy analyzer[34] demonstrated that the spread in ion kinetic energy was not more than a few volts.

The distribution in the directions of the ions leaving the accelerator grid results in a gradual spreading of the stream with distance down the chamber. The radial space-charge field also contributed to this spreading. Figure 3 shows a series of ion density profiles transverse to the flow at several axial positions in a stream originating from a 2.5-cm-diam grid. The stream spreads out to virtually fill the chamber at the end of the test section. The radial gradients are sufficiently small near the axis for the stream to be regarded as approximately uniform for models several centimeters in diameter. The stream density drops approximately as the inverse square of the distance from the source, in the manner expected for constant velocity, source-like flows. A typical trace of centerline ion density down the chamber is shown in Fig. 4.

The continuity equation was applied to a profile of stream density similar to Fig. 3 to obtain the ion streamline pattern shown in Fig. 5. This pattern has also been verified using

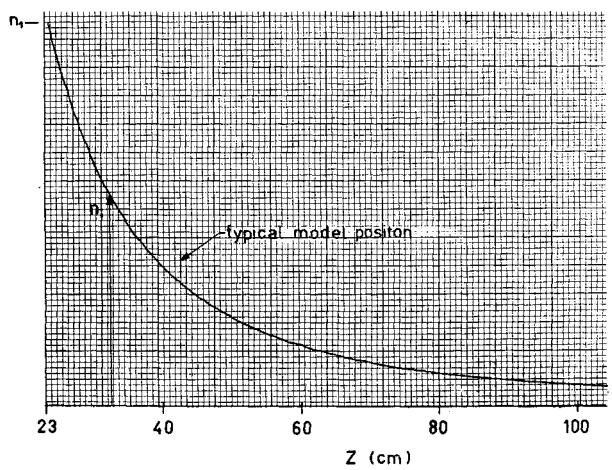

Fig. 4 Distribution of ion density down the centerline of the stream shown in Fig. 3; $n_1 = 1.4 \times 10^8$ cm^{-3}.

Table 2 Arrangement of equipment in wake studies

Figure no.	Model radius a (cm)	Source radius R_s (cm)	Source-model distance, Z (cm)
8	0.35	1.27	42
9	1.27	5	23
10–13	1.27	1.27	42
14	2.54	1.27	42
16	1.27	10	23

the directional sensitivity of the Langmuir probe under ionospheric flow conditions.[25] The ion streamlines curve outward slightly due to the radial electric field present where the stream is not uniform. To a good approximation, however, they may be regarded as straight lines from the source. The divergence of the stream may cause the model wake features to be somewhat displaced from where they would be in a uniform stream.

In the ionosphere the ions possess a Maxwellian velocity distribution and therefore a well-defined temperature. In the plasma wind tunnel the distribution in the component of ion velocity transverse to the flight direction arises from the unequal deflection of the individual ions as they pass through the accelerator grid rather than from interparticle collisions. This velocity distribution is not, in general, easily calculated, since it depends on the electric field structure around the accelerator grid and this varies with the operating conditions. However, *far from the source* (as measured in units of the grid radius R_s), the transverse velocity distribution can be estimated and an equivalent mean thermal speed defined.

Figure 6 shows a sketch of the ion trajectories that can reach a point near the stream axis a distance Z downstream of the source ($Z/R_s \gg 1$). The maximum transverse velocity with respect to the local stream direction that an ion reaching this point can have is

$$V_{\max} \approx U \tan^{-1}(R_s/Z) \tag{3}$$

If all the ions which reach the point under consideration have very small deflection angles, i.e., if $\tan^{-1}(R_s/Z)$ is sufficiently small, it is reasonable to assume that ions from all points on the grid are equally likely to reach this point in the stream (in other words, one assumes that the probability that an ion is deflected through a certain angle as it passes through the grid is the same for all sufficiently small angles). With this assumption, one can readily derive an expression for the transverse velocity distribution of the ions at a point near the stream axis. For a circular grid, the transverse velocity distribution function in one dimension is obtained as

$$F(V) = (2/\pi V_{\max})[1 - (V/V_{\max})^2]^{1/2} \tag{4}$$

where V represents the ion velocity component in a particular direction transverse to the flow, and $F(V)dV$ represents the fraction of ions at point z with transverse velocity between V and $V + dV$.

From Eq. (4), one finds that the average magnitude of V is

$$|\overline{V}| \simeq (4/3\pi)(R_s U/Z) \tag{5}$$

In a Maxwellian distribution, the average magnitude of the component of the thermal velocity in a particular direction is one half the average thermal speed. We therefore estimate an effective ion thermal speed by setting

$$\bar{c}_i = 2|\overline{V}| = (8/3\pi)(R_s U/Z) \tag{6}$$

It is clear from the assumptions involved that Eq. (6) represents an upper bound for $\bar{c}_i$, but should yield a good estimate when $Z \gg R_s$ (i.e., $\bar{c}_i \ll U$), as was the case in most of the experiments described below (Table 2 lists the values of R_s and Z). For $\bar{c}_i \sim U$, however, the estimate is open to question.

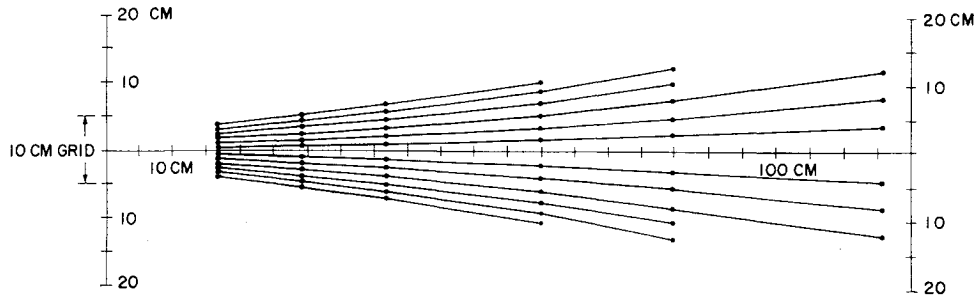

Fig. 5 Ion stream line pattern in plasma stream.

Nevertheless, in all cases, where $\bar{c}_i$ is mentioned below, it has been estimated from Eq. (6).

In a facility of this sort there are, in addition to the stream ions, ions which have been produced by charge exchange collisions between the high energy stream ions and the neutral gas in the test chamber. The slow ions produced in this way have a much longer residence time in the stream than the stream ions, and hence even when only a very small fraction of the stream ions suffer charge exchange collisions, the density of slow ions may be a significant fraction of the stream ion density. The presence of an excessive proportion of slow ions has been a serious drawback in previous facilities[22,24] intended for the study of ionospheric plasma flows. In our facility a large diffusion pump was employed to lower the chamber pressure, and the open area of the accelerator grid was limited in order to reduce the effusion of neutral atoms from the ionization chamber. This neutral effusion accounts for most of the mass flow and thus limits the vacuum chamber pressure.

The density of slow charge exchange ions can in principle be estimated from a balance of the rates of production and loss. Unfortunately, the rate of loss is not easily estimated. Clayden and Hurdle[22] and Sajben and Blumenthal[24] have suggested various estimates of the loss rate. The highest estimate predicts a background density of about 1% of the stream density for our typical operating conditions, and the lowest estimate predicts about 10%. Our own measurements favor the lower figure for background density.

The slow ion density was measured in the present facility by two methods. In the first, the electron density was measured (from the electron current to a probe at local plasma potential) in that part of the near wake of a model which is inaccessible to stream ions. This density should represent an upper limit for the possible slow ion density in the freestream. The second indication used was the ion collection of a plate shielded from direct impingement by the stream ions. The plate formed the bottom of a cup oriented transverse to the flow direction. The background ion density was estimated from the formula for the saturation ion current drawn by the plate,

$$I \sim en_b(kT_e/m_i)^{1/2}A \qquad (7)$$

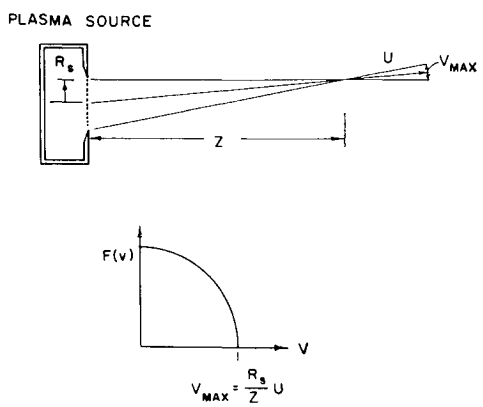

Fig. 6 Transverse velocity distribution of stream ions.

where the actual plate area was used for the collection area A in order to obtain an upper bound on the background ion density.

The results of these measurements are plotted in Fig. 7. The background density is expected to be linearly related to neutral gas pressure for constant stream conditions, hence a line of unit slope is drawn through the data on the log-log plot. Under normal operating conditions in the experiments described in the following section, the background ion density was a few percent of the stream ion density, according to the results.

3. Measurements of Wake Structure and Discussion

This section describes a series of wake measurements of bodies (mostly spheres) which are moderate or large in size compared with the Debye length. All of the data are for the case of zero magnetic field, and most for cold ions, $T_i/T_e \ll 1$, although some examples with significant ion thermal motion are also shown (only where explicit mention of $\bar{c}_i(kT_e/m_i)^{-1/2}$ is made is that ratio comparable with unity). The speed ratio $U(kT_e/m_i)^{-1/2}$ in these tests was in the neighborhood of 10. The exact values are given in the figure captions, together with other pertinent data.

Profiles of ion density through wakes are shown in Figs. 8–17. In the figures, z represents the distance measured downstream from the rear of the model in the flow direction, and x the distance from the axis in the transverse direction. Raw data of ion current (proportional to ion density), obtained directly from the recorder, show some of the radial nonuniformity of the stream. Some data (Figs. 8, 9, 14, and 16) have been replotted to show only the fractional difference of the ion density from that of the undisturbed stream in the absence of the model. To give the reader an idea of the axial gradients, two values of a/λ_D are given in each figure caption, one specifying the condition at the model and the other representing the value at the station of the furthest downstream ion density traverse. Further information on the model radius, axial position of model, and accelerator grid size (related to the effective ion temperature, as described in the previous section) is provided in Table 2.

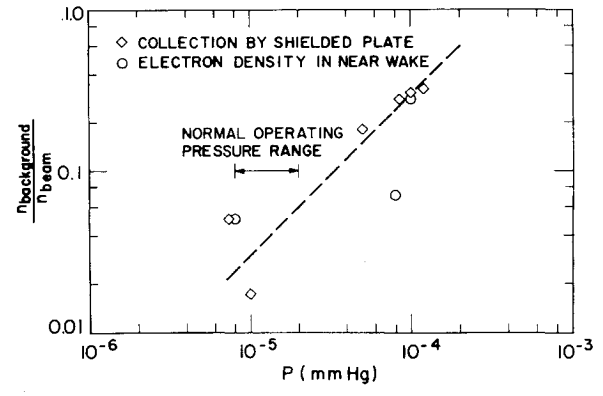

Fig. 7 Density of slow background ions in the plasma stream.

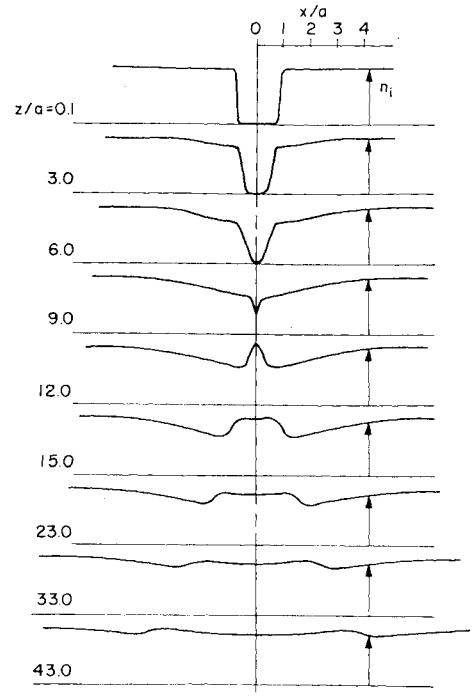

Fig. 8 Wake of a floating cylinder; $U(kT_e/m_i)^{-1/2} = 9$, $a/\lambda_D = 1.6$ at model and 1.2 at last trace, $e\phi_\sigma/kT_e = -3.5$.

Figure 8 shows the wake of a cylinder with radius only somewhat larger than the Debye length. The body sweeps out the ions from the stream and leaves a void immediately behind it. The ions stream into this void, partly because they are deflected inward as they pass through the sheath around the negatively charged body, and partly because they are attracted by the negative space charge which results from the penetration of the higher energy electrons into the wake region. (Thermal motion also contributes to this process when the ions are not cold.) For bodies small compared with the Debye length, the deflection in the sheath is the primary effect, but the influence of the space-charge field increases with body size, and dominates for bodies very large compared with the Debye length. The wake shown in Fig. 8 is intermediate (in terms of Debye length to body radius) to the wakes of fine

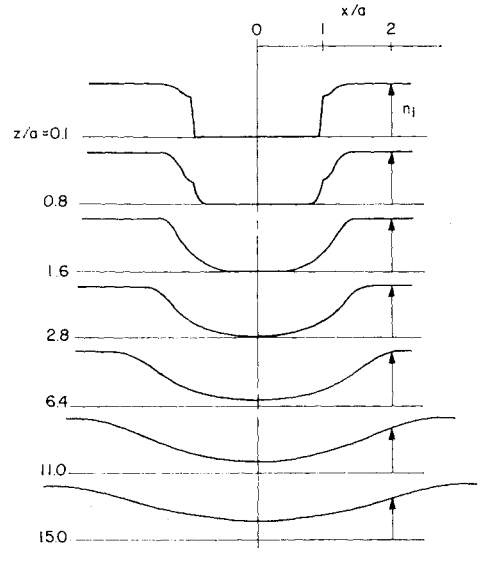

Fig. 9 Ion density distribution in the wake of a flat strip transverse to the ion stream; $U(kT_e/m_i)^{-1/2} = 15$, $a/\lambda_D = 40$ at model and 24 at last trace, $e\phi_\sigma/kT_e = -3$, $\bar{c}_i(kT_e/m_i)^{-1/2} \sim 1$.

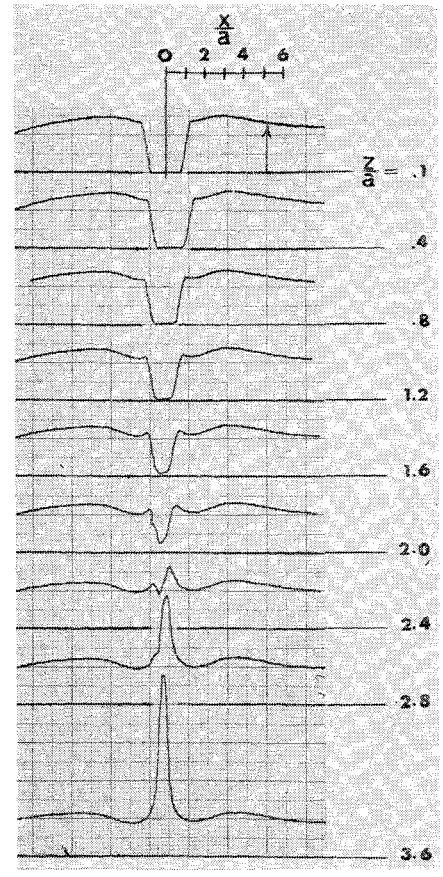

Fig. 10 Ion density in the wake of a floating sphere; $U(kT_e/m_i)^{-1/2} = 8$, $a/\lambda_D = 1.8$ at model and 1.4 at last trace, $e\phi_\sigma/kT_e = -3.5$.

wires and the wakes of large cylinders described by the authors elsewhere (Refs. 29 and 25, respectively).

In Fig. 8, the ion streams are deflected by the body, converge onto the centerline where they meet and the densities of the two streams add to form a peak, and then the deflected streams pass through each other and continue into the plasma on the opposite side of the wake centerline. At the same time a rarefaction wave is generated at the body and moves into the undisturbed plasma on both sides at an inclination of about the Mach angle, $\sin^{-1}[(kT_e/m_i)^{1/2}/U]$.

Taylor[13] has calculated the wake of a bar with half-width $1.5\lambda_D$ and thickness in the stream direction $0.6\lambda_D$ in a plasma where the ion and electron temperatures are equal. The speed ratio was $U(kT_e/m_i)^{-1/2} = 8.5$ and the wake structure was calculated for two body potentials ($e\phi_\sigma/kT_e = -2.75$ and $e\phi_\sigma/kT_e = -14$). His results are qualitatively similar to the wake of Fig. 8. His computations show a dependence of the wake angle on body potential, as one would expect if the wake is formed by the ion streams which are deflected across the wake centerline. Call[35] has made a computation of the wake of a strip of half-width $1.0\ \lambda_D$ in a cold ion stream with $U(kT_e/m_i)^{-1/2} = 5$ for two different body potentials ($e\phi_\sigma/kT_e = 0$ and $e\phi_\sigma/kT_e = -5$). These calculations also show similar wake features and demonstrate the wake angle dependence on body potential.

The near wake of a large strip (with a thickness to half-width ratio of 0.005) transverse to the flow direction is illustrated in Fig. 9. The model was placed relatively near a large accelerator grid, so that the effective ion temperature was not small compared with the electron temperature. In this case the ion deflection by the sheath around the body is much less important in the wake filling than the negative space-charge potential in the near wake and the thermal motion of the ions. As the plasma expands to fill the void behind the body, a rare-

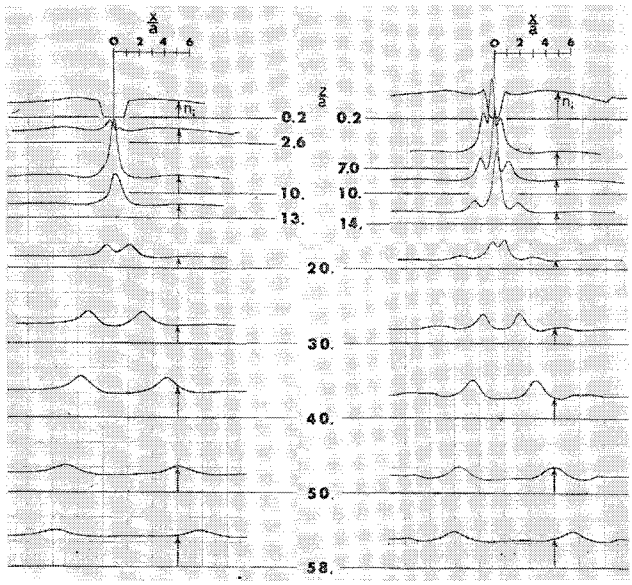

Fig. 11 Far wake of a sphere when floating and when negatively biased; $U(kT_e/m_i)^{-1/2} = 8$, $a/\lambda_D = 1.8$ at model and 0.7 at last trace; $e\phi_\sigma/kT_e = -3.5$ at left, $e\phi_\sigma/kT_e = -20$ at right.

faction wave, essentially quasineutral, advances into the undisturbed plasma stream at an inclination approximately equal to the Mach angle based on the plasma wave speed, as in the theory of Lam and Greenblatt.[36]

The near wake of an electrically floating sphere with a radius of 1.8 Debye lengths is shown in Fig. 10. The ions are deflected toward the wake axis by the inwardly directed force field around the body and in the near wake. When the ion streams meet on the wake axis, a strong density peak appears. The remarkable strength of this peak arises from the focussing effect of this axisymmetric geometry and from the low ion temperature which tends to minimize dispersion by thermal motion. The near wake of Fig. 10 is in qualitative agreement with applicable theory.[11,12]

Fig. 11a takes the wake of Fig. 10 to distances further downstream. The strong peak on the wake axis is seen to divide into a cylindrically symmetric outward moving peak. The shape of the peak is substantially preserved as the wake develops, although some additional structure appears in the interior portion of the wake.

It is of some interest to inquire whether this outward moving density peak is made up of a group of ions which were deflected across the wake axis, as in the cylinder wakes, and are moving outward through a largely undisturbed background plasma, or whether the peak is more like a wave propagating through the collective interaction of all the plasma through which it passes. In order to try to answer this question, the influence of body potential on the wake structure was investigated. If the structure is simply due to ion streams which have been deflected across the wake axis, then increasing the amount of the stream deflection should result in a larger wake angle, as in the wakes of small wires.[29] If, however, the structure is due to a wavelike behavior, then the wake angle should be primarily a function of the flow conditions and should not be increased by an increase of the stream deflection.

Figure 11b shows the wake structure for the same flow conditions as in Figs. 10 and 11a, but here the body potential is highly negative. A stronger density peak is observed behind the body than in the previous case. A small cylindrical peak separates from the central peak and moves rapidly outward. This is presumably made up of ions which passed through the sheath around the body, were deflected across the axis, and continue to stream outward. This possibility is supported by the fact that the peak amplitude drops approximately as the inverse of its distance from the wake axis. Further downstream, the main central peak itself divides into a cylindrical outward moving disturbance, very much as in the case of the lower potential. In fact, far downstream the width of the wake in Fig. 11b is actually less than that of Fig. 11a. However, the slope of the advancing front is approximately equal to the Mach angle, $\sin^{-1}[U(kT_e/m_i)^{-1/2}]$ in both cases.

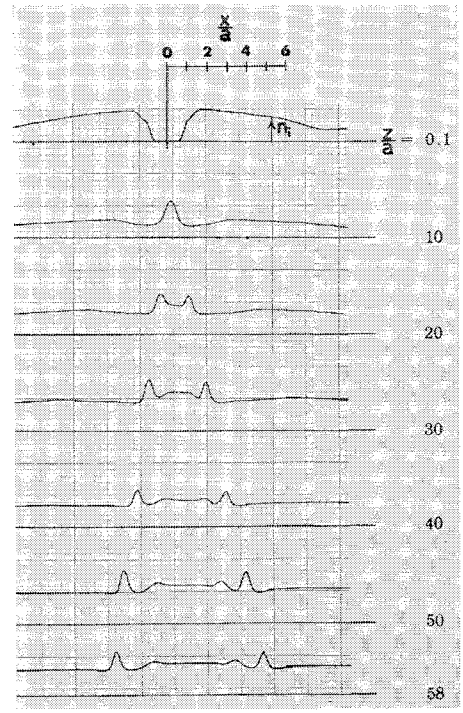

Fig. 12 Far wake of a larger floating sphere; $U(kT_e/m_i)^{-1/2} = 11.5$, $a/\lambda_D = 7$ at model and 2 at last trace, $e\phi_\sigma/kT_e = -3.5$.

Figure 12 shows the wake of a somewhat larger sphere, with more strongly developed features. Figure 13a shows the details of this wake at a station far downstream, and Figure 13b shows how the wake structure at that station changes when the sphere potential is changed from -3.5 to -30 dimensionless units. Clearly, the dependence on body potential is minor. The wake width is merely somewhat less in the higher potential case.

The wake of a still larger sphere, with $a/\lambda_D = 14$, is shown on Fig. 14. This figure also includes profiles of plasma potential obtained with an emissive probe.

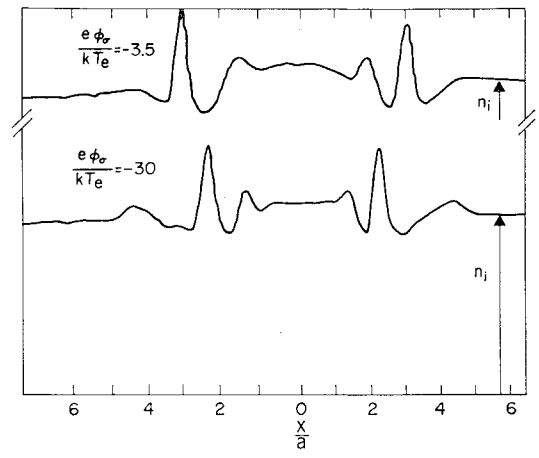

Fig. 13 Effect of body potential on wake profile at $z/a = 58$ under flow conditions of Fig. 12; $e\phi_\sigma/kT_e = -3.5$ (as in Fig. 12), and $e\phi_\sigma/kT_e = -30$.

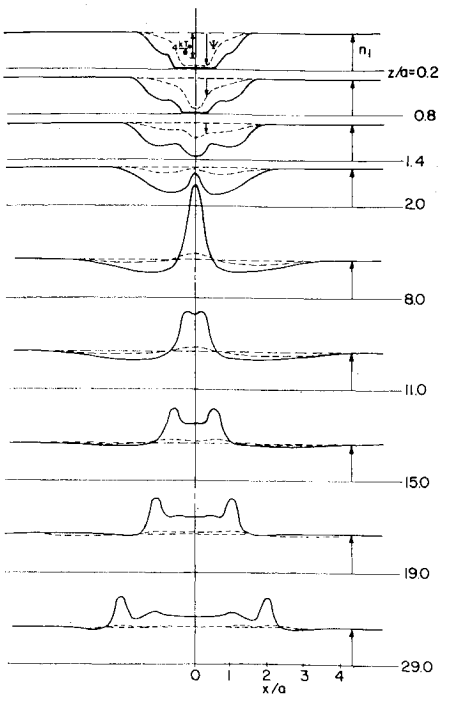

Fig. 14 Ion density and plasma potential in the far wake of a large sphere; $U(kT_e/m_i)^{-1/2} = 10.5$, $a/\lambda_D = 14$ at model and 5 at last trace, $e\phi_\sigma/kT_e = -3.5$.

We are led to conclude that the far wake of a spherical body has a wavelike character; that is, the disturbance propagates through the collective interaction of all the plasma through which it passes, moving at the ion acoustic speed, rather than as a pseudowave in which the ions stream through an essentially undisturbed background plasma.

The following picture emerges of the wake of a sphere. The inwardly directed electric field in the sheath and near wake deflects the ions toward the wake axis, the deflection being greatest for those ions which pass closest to the sphere and progressively less for those which pass at larger distances. As the ions arrive at the axis a density peak, and with it a positive potential peak, builds up. The first ions will always cross the axis (e.g., Fig. 11b), but the ones arriving further downstream possess progressively less inwardly directed kinetic energy, and at some point downstream the ions will be turned back by the potential peak before reaching the axis. At about this point the peak on the axis will start to divide into a cylindrical outward moving peak. (This picture of the initial wake formation is also shown clearly in the theoretical calculations of Maslennikov and Sigov.[11]) Our experiments suggest that downstream of this point, the

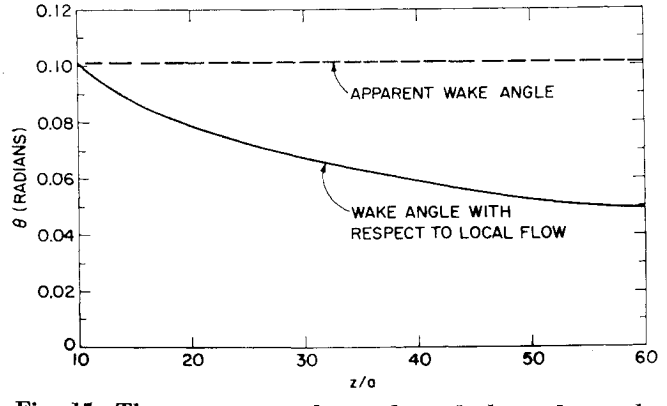

Fig. 15 The apparent wake angle and the wake angle with respect to the local streamline direction, for wake of Fig. 12.

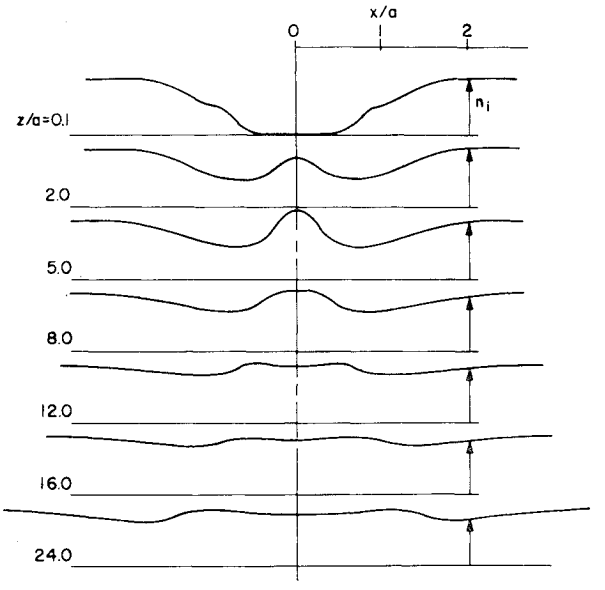

Fig. 16 Far wake of a sphere in temperate plasma; $U(kT_e/m_i)^{-1/2} = 9$, $a/\lambda_D = 10$ at model and 6 at last trace, $e\phi_\sigma/kT_e = -3.5$, $\bar{c}_i(kT_e/m_i)^{-1/2} \sim 1$.

wake has a predominantly wavelike character. The mean features are carried at approximately the Mach angle based on the ion acoustic speed, and are not dominantly influenced by Debye length or body potential, even for spheres with radii as small as a Debye length.

For the more strongly biased spheres, the division of the axial peak occurs somewhat further downstream (Fig. 11) apparently because with a greater initial deflection, the point at which the central potential peak reaches sufficient strength to stop the inward motion occurs further downstream. Since the wavelike structure of the far wake starts at this point, the wake of a more highly biased body is actually somewhat narrower at a given downstream station, as shown in the figures.

We note that it is the axisymmetry of the sphere wake which results in conditions favorable for a wave behavior in the far wake. Experiments have shown[29] that for cylinders (at least for those comparable with or smaller than the Debye length) the far wake is dominated by those ions which were deflected across the stream centerline in the near wake, and wake angle

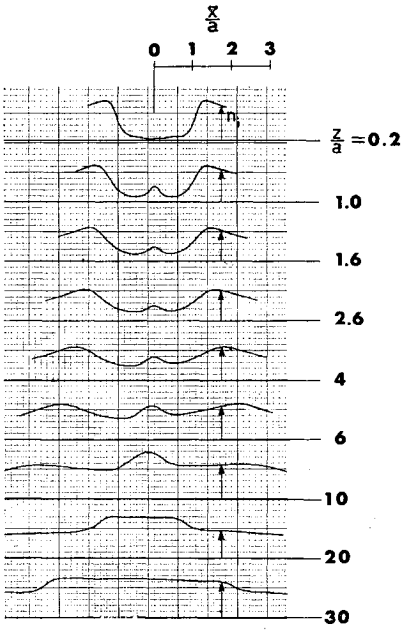

Fig. 17 Far wake of large sphere in temperate plasma; $U(kT_e/m_i)^{-1/2} = 7$, $a/\lambda_D = 46$ at model and 14 at last trace, $e\phi_\sigma/kT_e = -3.5$, $\bar{c}_i \times (kT_e/m_i)^{-1/2} \sim 1$.

is dependent on a/λ_D and body potential and is not in general equal to the Mach angle. (Note that approximate theories have been formulated which imply far wakes oriented at the Mach angle for both spheres and cylinders.[1,6,7])

The fact that the wake angle for the sphere far wake was virtually constant and to a good approximation equal to the Mach angle is actually somewhat surprising, since the wake is formed in the diverging source-like ion stream of the wind tunnel. In such a flow disturbance which moves outward at the ion wave speed with respect to the local plasma would give rise to a wake angle which increases with distance downstream from the body. In Fig. 15, we compare the apparent far wake angle of Fig. 12 as measured with respect to the flow axis with the wake angle relative to the local flow direction. (The latter is calculated by assuming rectilinear ion trajectories from the source, so that

$$\theta_{\text{corrected}} = \theta_{\text{apparent}} - \tan^{-1}(r/Z) \tag{8}$$

where r is the radial distance from the stream axis, and Z is the distance downstream from the source.) The wake angle with respect to the local flow starts at about the Mach angle and then decreases gradually to about half its initial value at the furthest downstream measurement. This result may be due to the stream divergence, in which case it would not occur in the ionosphere where the flow is uniform. It is possible that the source-like flowfield may contribute to some details of the observed far wake structure.

Finally, the effect of ion thermal motion on the wake of a sphere is illustrated in Figs. 16 and 17. A qualitative similarity with the cold ion wakes persists, but the thermal motion enhances the rate of wake filling, reduces the magnitude of the ion density peaks, and generally moderates the sharp features observed in a cold plasma. We would caution the reader against reading too much detail from these wakes, however, since the ion velocity distribution was not Maxwellian and our estimate for the effective $\bar{c}_i$ is in this case only an upper bound (see Sec. 2).

4. Conclusions

The experiments described here have revealed some of the basic features of the wakes of bodies in hypersonic, collisionless plasma flows. The wavelike nature of the far wakes of spheres is, to the author's knowledge, demonstrated experimentally here for the first time. Although these experiments were performed in the absence of a magnetic field and in most cases in a cold ion plasma, the results are expected to be fundamentally pertinent to the problem of the disturbance caused by a satellite in the earth's ionosphere.

References

[1] Al'pert, Ya. L., Gurevich, A. V., and Pitaevskii, L. P., *Space Physics with Artificial Satellites*, Consultants Bureau, New York, 1965.

[2] Bourdeau, R. E., "Ionospheric Research from Space Vehicles," *Space Science Reviews*, Vol. 1, 1962–1963, pp. 683–728.

[3] Samir, U. and Wrenn, G. L., "The Dependence of Charge and Potential Distribution around a Spacecraft on Ionic Composition," *Planetary and Space Science*, to be published.

[4] Singer, S. F., *Interaction of Space Vehicles with an Ionized Atmosphere*, Pergamon Press, New York, 1967.

[5] deLeeuw, J. H., "A Brief Introduction to Ionospheric Aerodynamics," *Rarefied Gas Dynamics*, Suppl. 4, Vol. II, edited by C. L. Brundin, Academic Press, New York, 1967, pp. 1561–1586.

[6] Kraus, L. and Watson, K. M., "Plasma Motion Induced by Satellites in the Ionosphere," *The Physics of Fluids*, Vol. 1, No. 6 Nov.–Dec. 1958, pp. 480–488.

[7] Rand, S., "Wake of a Satellite Traversing the Ionosphere," *The Physics of Fluids*, Vol. 3, No. 2, March–April 1960, pp. 265–273.

[8] Rand, S., "Damping of the Satellite Wake in the Ionosphere," *The Physics of Fluids*, Vol. 3, No. 4, July–Aug. 1960, pp. 588–599.

[9] Davis, A. H. and Harris, I., "Interaction of a Charged Satellite with the Ionosphere," *Rarefied Gas Dynamics*, Suppl. 1, edited by L. Talbot, Academic Press, New York, 1961, pp. 691–699.

[10] Sawchuck, W., "Wake of a Charged Prolate Spheroid at an Angle of Attack in a Rarefield Plasma," *Rarefied Gas Dynamics*, Suppl. 2, Vol. II, edited by J. A. Laurmann, Academic Press, New York, 1963, pp. 33–44.

[11] Maslennikov, M. V. and Sigov, Yu. S., "Discrete Model of Medium in a Problem on Rarefied Plasma Stream Interaction with a Charged Body," *Rarefied Gas Dynamics*, Suppl. 4, Vol. II, edited by C. L. Brundin, Academic Press, New York, 1967, pp. 1657–1670.

[12] Maslennikov, M. V. and Sigov, Yu. S., "Plasma Stream Interaction with Charged Bodies of Various Forms," *Rarefied Gas Dynamics*, Suppl. 5, Vol. II, edited by L. Trilling and H. Wachman, Academic Press, New York, 1969, pp. 1671–1680.

[13] Taylor, J. C., "Disturbance of a Rarefied Plasma by a Supersonic Body on the Basis of the Poisson-Vlasov Equations-I," *Planetary and Space Science*, Vol. 15, 1967, pp. 157–187.

[14] Taylor, J. C., "Disturbance of a Rarefied Plasma by a Supersonic Body on the Basis of the Poisson-Vlasov Equations-II," *Planetary and Space Science*, Vol. 15, 1967, pp. 463–474.

[15] Kiel, R. E., Gey, F. C., and Gustafson, W. A., "Electrostatic Potential Fields of an Ionospheric Satellite," *AIAA Journal*, Vol. 6, No. 4, April 1968, pp. 690–694.

[16] Liu, V. C. and Jew, H., "Near Wake of the Rarefied Plasma Flows at Mesothermal Speeds," AIAA Paper 68–169, New York, 1968.

[17] Hohl, F. and Wood, G. P., "Electrostatic and Electromagnetic Drag Forces on a Spherical Satellite in a Rarefied Partially Ionized Atmosphere," *Rarefied Gas Dynamics*, Suppl. 2, Vol. II, edited by J. A. Laurmann, Academic Press, New York, 1963, pp. 45–64.

[18] Shea, J. J., "Collisionless Plasma Flow Around a Conducting Sphere in a Magnetic Field," *Rarefied Gas Dynamics*, Suppl. 4, Vol. II, edited by C. L. Brundin, Academic Press, New York, 1967, pp. 1671–1686.

[19] Pan, Y. S. and Vaglio-Laurin, R., "Trail of an Ionospheric Satellite I," *AIAA Journal*, Vol. 5, No. 10, Oct. 1967, pp. 1801–1810; also "Trail of an Ionospheric Satellite II," *Rarefied Gas Dynamics*, Suppl. 4, Vol. II, edited by C. L. Brundin, Academic Press, New York, 1967, pp. 1687–1702.

[20] Meckel, B. B., "Experimental Study of the Interaction of a Moving Body with a Plasma," *Rarefied Gas Dynamics*, Suppl. 1, edited by L. Talbot, Academic Press, New York, 1961, pp. 701–714.

[21] Hall, D. F., Kemp, R. F., and Sellen, J. M., Jr., "Plasma-Vehicle Interaction in a Plasma Stream," *AIAA Journal*, Vol. 2. No. 6, June 1964, pp. 1032–1039.

[22] Clayden, W. A. and Hurdle, C. V., "An Experimental Study of Plasma-Vehicle Interaction," *Rarefied Gas Dynamics*, Suppl. 4, Vol. II, edited by C. L. Brundin, Academic Press, New York, 1967, pp. 1717–1731.

[23] Skvortsov, V. V. and Nosachev, L. V., *Cosmic Investigations*, Vol. 6, p. 228, 1968 (in Russian).

[24] Sajben, M. and Blumenthal, D. L., "Experimental Study of a Rarefied Plasma Stream and Its Interaction with Simple Bodies," AIAA Paper 69–79, New York, 1969.

[25] Hester, S. D. and Sonin, A. A., "Some Results from a Laboratory Study of Satellite Wake Structure and Probe Response in Collisionless Plasma Flows," *Rarefied Gas Dynamics*, Suppl. 5, Vol. II, edited by L. Trilling and H. Wachman, Academic Press, New York, 1969, pp. 1659–1670.

[26] Henderson, C. L. and Samir, U., "Disturbed Region about an Ionospheric Satellite," *Planetary and Space Science*, Vol. 15, 1967, pp. 1499–1513.

[27] Samir, U. and Willmore, A. P., "The Distribution of Charged Particles near a Moving Spacecraft," *Planetary Space and Science*, Vol. 13, 1965, pp. 285–296; also, "The Equilibrium Potential of a Spacecraft in the Ionosphere," *Planetary and Space Science*, Vol. 14, 1966, pp. 1131–1137.

[28] Medved, D. B., "Measurement of Ion Wakes and Body Effects with the Gemini/Agena Satellite," *Rarefied Gas Dynamics*, Suppl. 5, Vol. II, edited by L. Trilling and H. Wachman, Academic Press, New York, 1969, pp. 1525–1540.

[29] Hester, S. D. and Sonin, A. A., "A Laboratory Study of the

Wakes of Small Cylinders under Ionospheric Satellite Conditions," *The Physics of Fluids*, Vol. 13, No. 3, March 1970, pp. 641–648.

[30] Hester, S. D. and Sonin, A. A., "Ion Temperature Sensitive End Effect in Cylindrical Langmuir Probe Response at Ionospheric Satellite Conditions," *The Physics of Fluids*, Vol. 13, No. 5, May 1970, pp. 1265–1274.

[31] Mickelson, W. R. and Kaufmann, H. R., "Present Status of Electron Bombardment Ion Rockets," TND 2172, 1964, NASA.

[32] Chen, F. F., "Electric Probes," *Plasma Diagnostic Techniques*, edited by R. H. Huddleston and S. L. Leonard, Academic Press, New York, 1965, pp. 113–200.

[33] Sonin, A. A., "Free-Molecule Langmuir Probe and Its Use in Flow Field Studies," *AIAA Journal*, Vol. 4, No. 9, Sept. 1966, pp. 1588–1596.

[34] Simpson, J. A., "Design of Retarding Field Energy Analyzers," *Review of Scientific Instruments*, Vol. 32, No. 12, Dec. 1961, pp. 1283–1293.

[35] Call, S., Ph.D. thesis, 1968, Columbia Univ.

[36] Lam, S. H. and Greenblatt, M., "On the Interaction of a Solid Body with a Flowing Collisionless Plasma," *Rarefied Gas Dynamics*, Suppl. 3, Vol. II, edited by J. H. deLeeuw, Academic Press, New York, 1966, pp.45–61.

JUNE 1970 AIAA JOURNAL VOL. 8, NO. 6

Electrostatic Field in the Trail of Ionospheric Satellites

R. Vaglio-Laurin* and G. Miller†
New York University, Bronx, N. Y.

Conceptual similarities between the electrostatic near wake of an ionospheric satellite and the fluid-dynamic near wake of a blunt-base body in low-speed flow are noted. A simplified model of the electrostatic wake is constructed accordingly. There are recognized distinct regions where different approximate solutions of the Poisson equation are valid, namely: 1) an outer region, conceptually analogous to the external inviscid flow, where the self-induced electric field due to the charge separation develops independently of the boundary conditions on the body; 2) an inner region, analogous to the recirculation zone, where the electric field configuration is largely governed by the vehicle shape, whereas the field intensity is controlled by the flight condition (the ion Mach number) and by the difference between the body floating potential and the minimum potential characteristic of the flow; 3) an intermediate region, analogous to the fluid-dynamic free shear layer, where a rapid adjustment between the two aforenoted solutions is attained. Analyses appropriate to the various regions are presented and their combination to obtain a composite solution is described. The merit of the model resides in its ability to provide rapid estimates of the electrostatic wake; its validity is corroborated by heuristic arguments as well as by comparisons with the results of numerical solutions for axisymmetric configurations.

I. Introduction

A DETAILED knowledge of flowfields around ionospheric satellites is required in many data reduction problems, e.g., the interpretation of on-board measurements and of radar observations, the calculation of drag, etc. The gross features of the flow can easily be identified by considering the set of parameters characteristic of the physical processes in the plasma, by comparing their relative magnitudes in the situation of interest, and by determining accordingly the dominant physical effects. However, detailed analysis remains rather elaborate, particularly with regard to the charged components of the gas in the trail where self-induced electric fields and externally imposed magnetic fields dominate the behavior of charged particles over regions having extent comparable to or larger than the typical vehicle dimension.

The interaction between satellites and charged particles in the ionosphere has received considerable attention in recent years[1,2]; as a result, the roles of electrostatic and magnetostatic fields are understood. For typical ionospheric conditions (altitudes between 150 and 1500 km) and typical vehicle dimensions of the order of meters, the effect of the magnetic field is manifested mainly in the structure and decay of the far trail,[1,3,4] whereas the effect of the electric field is confined to a thin Debye sheet on the windward side of the vehicle, and to a near trail region, hereafter called the electrostatic wake, on the leeward side.[1,5–7] The transversal scale of the electrostatic wake is comparable to the typical body dimension a, while its streamwise scale is of the order of $M_i a$, M_i being the ion Mach number.

The present paper is concerned with the electrostatic wake in the context of the simplified over-all description of the trail initiated in Refs. 3 and 4. Specific attention is devoted to the extension of previous physical-analytical models[1,7] with a view toward obtaining improved agreement between approximate analysis and the results of numerical solutions of the governing equation[5,6] (the Poisson equation). The formulation of the model is guided by several conceptual similarities between the present problem and the fluid-dynamic near wake downstream of a blunt-base body in low-speed flow. In this vein the electrostatic wake is divided in distinct regions where different approximate solutions of the Poisson equation are valid. Broadly, the regions represent the counterparts of the external inviscid flow, the free shear layer and the recirculation zone.

The paper touches on various aspects of the investigation in the following sequence: upon a brief restatement of the problem and a heuristic justification of the model (Sec. 2),

Presented as Paper 69-674 at AIAA Fluid and Plasma Dynamics Conference, San Francisco, Calif., June 16–18, 1969; submitted June 23, 1969; revision received November 12, 1969. The paper is based on research sponsored by U.S. Air Force Office of Scientific Research (OAR) under Grant AF-AFOSR 68-1551. The analysis of the free Debye layer (outer region) is extracted from a dissertation submitted by one of the authors, G. Miller, to the Faculty of the Graduate School of Engineering and Science in partial fulfillment of the requirements for the degree of Doctor of Philosophy at New York University.

* Professor.
† Assistant Professor.